Black raspberry modulates cecal and oral microbiome at the early stage of a dibenzo[def,p]chrysene-induced murine oral cancer model

Jingcheng Zhao[1], Yuan-Wan Sun[2], Kun-Ming Chen[2], Cesar Aliaga[2], Jordan E. Bisanz[1,3], Karam El-Bayoumy[2,*]

[1]Department of Biochemistry and Molecular Biology, Pennsylvania State University, University Park, Pennsylvania, USA; [2]Department of Biochemistry and Molecular Biology, Pennsylvania State University, College of Medicine, Hershey, PA 17033; [3]One Health Microbiome Center, Huck Life Sciences Institute, University Park, Pennsylvania, USA

Running title: Black raspberry, microbiome, and DBP-induced OSCC

* Corresponding Author
Dr. Karam El-Bayoumy, Department of Biochemistry & Molecular Biology, Pennsylvania State University, College of Medicine, 500 University Drive, Hershey PA, USA Phone: 717-531-1005 Email: kee2@psu.edu

Conflict of Interest: The authors declare no potential conflicts of interest.

ABSTRACT

While tobacco smoking is a risk factor in the development of oral squamous cell carcinoma (OSCC), only a fraction of smokers develop the disease. Compelling evidence shows that microbial dysbiosis is associated with carcinogenesis, suggesting that the microbiome may play a role in cancer development of smokers. We previously showed that black raspberry (BRB) protects against OSCC induced by the tobacco constituent dibenzo[def,p]chrysene (DBP) altering genetic and epigenetic markers in a manner consistent with its cancer preventive activity. In the present study, we conducted a mouse experiment to investigate the effects of BRB and DBP individually and in combination on the oral and gut microbiota. DBP-induced DNA damage in the mouse oral cavity which is an essential step for the development of OSCC in mice. 16S rRNA gene sequencing revealed that BRB significantly increased microbial diversity and shifted microbiome composition in the gut and oral cavity, whereas DBP had no significant effect. In both gut and oral microbiota, *Akkermansia muciniphila* was significantly reduced after BRB treatment; however, this was not consistent with pure culture *in vitro* assays suggesting that the impact of BRB on *A. muciniphila* may be mediated through indirect mechanisms including the host or other microbes. Indeed BRB, but not DBP, was found to modulate the growth kinetics of human gut microbes *in vitro* including lactic acid bacteria and *Bacteroides* spp. The results of the current study further emphasize the interplay of microbiome and environmental factors in the development and prevention of OSCC.

Prevention Relevance

Our work clearly demonstrates the modulatory impact of Black Raspberry (BRB) on both gut and oral microbiomes within a dibenzo[def,p]chrysene (DBP)-induced oral squamous cell carcinoma (OSCC) mouse model and paves the way for future research examining a causal role of BRB-microbiota interactions at different stages of disease progression.

INTRODUCTION

Oral squamous cell carcinoma (OSCC) is the most common malignancy among head and neck squamous cell carcinomas (HNSCC) that occur in the oral cavity including the tongue, lip, floor of mouth, gingiva, and other parts of the mouth (1,2). When OSCC happens, oral functions including swallowing and speech are often adversely influenced (3). Additionally, many patients suffer from impaired life quality resulting from damaged facial functions after surgery. Overall, the 5-year survival rate of OSCC is approximately 60% and is significantly improved if diagnosed at an early stage (2). Early detection represents one of the most promising approaches in increasing survival and minimizing negative impacts on quality of life. Despite advances in diagnostic tools to characterize oral malignant lesions, the percentage of OSCC diagnosed at early stages has not been significantly improved as most of the patients are asymptomatic and mucosal precancerous changes may not be detected by visual inspection of the oral cavity (4).

Recent evidence has shown that alterations in the oral microbiome are associated with development of OSCC (5,6). Previous studies also demonstrated that periodontal pathogens *Fusobacterium nucleatum* and *Porphyromonas gingivalis* promote oral carcinogenesis (7,8). In the oral cavity, *Porphyromonas gingivalis* disrupts the equilibrium of the immunoinflammatory state and *Fusobacterium nucleatum* becomes opportunistically pathogenic, contributing to periodontal diseases (9,10). Oral microbes identified in patients with OSCC have been proposed as microbial biomarkers to develop strategies for diagnosis and treatment (6,11,12). Nevertheless, the investigation of the OSCC-associated microbiome has many challenges (13–15), including significant individual variation and heterogeneity between results of previous studies, as the highly personalized oral microbiome is influenced by both intrinsic and extrinsic factors such as age, gender, diet, and smoking (15–18).

Exposure to tobacco smoke, an established etiological factor for the development of OSCC (19,20), is known to impact the oral microbiota (21,22). Although changes in microbial diversity are contradictory across studies (23), it has been reported that *Proteobacteria, Atopobium* spp., and *Streptococcus* spp. are increased, whereas *Capnocytophaga* spp*., Peptostreptococcus* spp*., and Leptotrichia* spp. are decreased in smokers compared to non-smokers (22).

Similar to human OSCC (24,25), a tobacco smoke constituent dibenzo[def,p]chrysene (DBP) induces OSCC in female mice, that progresses from hyperplasia, through dysplasia and carcinoma *in situ* to OSCC (26,27). At termination of the bioassay, the incidence of each histological type was reported as: 33.3% (dysplasia/papilloma), 13.3% carcinoma *in situ*, 40% OSCC (28). No histological changes were observed at early time point (5-6 weeks); however, mice developed dysplasia and carcinoma *in situ*, at 15 and 22 weeks, respectively. We previously showed that DBP caused DNA damage and mutations in the murine oral cavity with profiles similar to those found in the *p53* gene in human HNSCC (28). Our studies also showed that the p53 and COX-2 proteins were upregulated (26), while the expression of the tumor suppressor p120ctn protein was reduced in DBP-induced OSCC; p120ctn cooperates with EGFR to promote carcinogenesis (29,30). DNA adducts derived from DBP in the buccal cells of smokers and DBP-induced epigenetic changes such as hypomethylation of *Fgf3* have been detected at early stage prior to the detection of any histological abnormality in the mouse oral cavity (31), further emphasizing the potential contribution of DBP in the development of OSCC.

The current gold standard for diagnosis of OSCC is scalpel-obtained biopsy followed by histological examination; however, this approach is not suitable for routine screening tests. Saliva is a readily available biological fluid and its collection is simple and non-invasive. Despite numerous reports suggesting oral microbiome as a potential tool for early detection of oral cancer, information regarding the role of oral microbiota in carcinogenesis is limited (32). There are two theories proposed in the

literature (33): 1. “Bacteria before tumor”, in which bacterial damage to the epithelial cells activates a cascade of inflammatory pathways, leading to cell replication and production of reactive oxygen species which in turn can lead to DNA damage and carcinogenesis; 2. “Bacteria after tumor”, where opportunistic bacteria are attracted to the hypoxic, hyper-vascularized tumor environment, and they sustain the progression of the unhealthy ecosystem (34). Since the shift in the microbiome at the tumor stage could be a consequence of cancer development, using our mouse model induced by the tobacco/environmental carcinogen DBP to induce OSCC can provide a realistic platform to examine the shift of the microbiome at early stage before the development of tumor with the ultimate goal of discovering biomarkers for early detection.

Recently, we discovered that dietary black raspberry (BRB) powder significantly reduced tumor incidence by attenuating DBP-induced DNA damage, strengthening DNA repair, and regulating epigenetics (35). BRB has been previously reported to alter gut microbiome composition and function (36), suggesting a potential role for microbiome alterations to contribute to the prevention of OSCC (37). Given gut and oral microbiota highly connect to and interact with each other (38), the oral-gut microbiome axis is a potential key player in the development and prevention of OSCC. In the current study, we used our well-established DBP-induced DNA damage mouse model that mimics human OSCC to interrogate interactions of the microbiota with DBP and BRB under a well-defined experimental condition. We specifically focused on an early stage of carcinogenesis wherein DNA damage has occurred, but before tumor development to understand how the microbiota, DBP, and BRB interact at this critical time window for the early detection and prevention of OSCC (27).

Materials and Methods

Animal experiments

Animal studies were conducted based on a previously established murine model utilizing a relevant tobacco smoke constituent DBP to induce OSCC (26). Our previous carcinogenesis and mechanistic studies using DBP and chemoprevention using BRB were performed in female mice. We also found that histological changes and molecular characteristics following DBP treatment in female mice mimic those found in human OSCC. Therefore, briefly female B6C3F1 mice **(Fig. 1a)** were treated by topical application into the oral cavity with DBP dissolved in DMSO (24 nmol, 3 times per week for 5-6 weeks). Mice were randomized into four groups (N=5 mice per group). The DMSO and DBP groups were fed an AIN-93 M diet (5% corn oil) as the control diet and received DMSO and DBP treatment, respectively. In contrast, the BRB and BRB+DBP groups respectively treated with DMSO and DBP were on an AIN-93M diet containing BRB powder (5% w/w) provided by Berri Products LLC. Previous evidence had indicated that 24 nmol, 3 times per week of DBP administration could induce DNA damage without causing any histological changes (26) and 5% was the optimal level of BRB to protect against tumor development in murine models (20). The mice were monitored weekly for any morphological abnormalities around the mouth and nose area and the body mass was recorded. One day after the last dose of carcinogen treatment, oral samples were collected by swabbing the oral cavity including the tongue, buccal areas, gingivae, and palate using ultra-fine polystyrene according to a published procedure (39). The cecal content was collected by using a sterile spatula to scrape the cecal content from the mouse cecum into a sterile tube on the same day. The oral tissues were harvested for DNA adduct analysis. Two mice from each group were euthanized at 5 weeks while the remaining three mice were euthanized at 6 weeks. At the end of week 5, our animal biologist was able to sacrifice 2 mice per group in one day and carefully, to avoid contamination (tedious process) collect oral and cecal samples as well as oral tissues for the analysis of DNA damage and microbiome analysis. At the beginning of week 6, 3 mice were sacrificed per group in one day and collection of samples was performed. Based

on our previous studies, maximum DNA damage was observed at 5 weeks. Furthermore, dietary changes can rapidly alter the microbiome within days and thus, a duration of 5 weeks is sufficient for observing a shift in microbiome following BRB administration. Therefore, we combined the microbiome data generated at both timepoints as indicated in Figure 1a. All samples were stored at -80°C until processing. The animal protocols were approved by the Institutional Animal Care and Use Committee (IACUC) at the Penn State College of Medicine.

Analysis of DNA adducts in oral tissues by LC-MS/MS

DBP is known to be metabolized to dibenzo[*a*,*l*]pyrene-11,12-dihydrodiol-13,14-epoxides (DBPDE) which can damage DNA and is a potent mutagen in both prokaryotic and eukaryotic *in vitro* systems (27). In this study, the oral tissues of mice were examined for the levels of DBPDE-dA (deoxyadenosine) adducts as reported previously by our team (26–28). In brief, DNA was isolated from oral tissues using a Qiagen DNA kit according to the manufacturer's manual. The internal standard [^{15}N5]- DBPDE-N^6-dA was added before DNA hydrolysis. After DNA samples were hydrolyzed by DNase I, phosphodiesterase, and alkaline phosphatase, an aliquot of the DNA hydrolysate was examined by HPLC to determine the levels of dA. The remaining hydrolysates were passed through an Oasis HLB column (1 ml, 30 mg; Waters Ltd.) before injection to HPLC for MS/MS analysis as described previously (31). The analysis was performed using a system consisting of Sciex QTRAP 6500+ mass spectrometry coupled with a Sciex EXion HPLC and equipped with a 1.7 µm Acquity UPLC BEH C18 analytical column (2.1 × 50 mm, Waters, Ireland). The mobile phase contained methanol/H_2O with the presence of 0.1% formic acid (flow rate = 0.3 ml/min) (31). The MS analysis was conducted by using a multiple reaction monitoring mode (MRM) with positive mode; the transitions of 604 → 335 and 609 → 335 were selected to quantify the DBPDE-N^6-dA and [^{15}N5]- DBPDE-N^6-dA, respectively. All peaks were integrated and quantified by Sciex OS 1.5 software.

DNA extraction

Oral and cecal samples were processed with a ZymoBIOMICS 96 MagBead DNA Kit (D4308) according to the manufacturer's instructions. A ZymoBIOMICS® Microbial Community Standard was used as a positive control to monitor DNA extraction efficiency and batch variation. Negative controls (i.e. blank extraction control, blank library preparation control) were included to assess the level of bioburden carried by the wet-lab process.

Amplicon library construction and 16S rRNA gene sequencing

The 16S rRNA gene sequencing was performed based on a previously established protocol (https://github.com/BisanzLab/AmpliconSeq). The primer pairs targeting the V4 region were used for primary PCR (40): Forward primer 515F (GTGYCAGCMGCCGCGGTAA) and reverse primer 806R (GGACTACNVGGGTWTCTAAT) with partial overhangs for i7 and i5 adapters. To obtain a late-exponential phase amplification for indexing, we made a series of 10x dilutions for amplification. KAPA HiFi hot start enzymes were used for amplification and SYBR green was applied to monitor the amplification progress. Next, the amplicons were diluted and dual-indexed with unique forward and reverse barcodes (12 nt). After indexing PCR, the amplification products were quantified by using Pico-green (Life Technologies) dye followed by pooling at equimolar concentrations to pursue even distributions of the reads among all samples. Then, the pooled samples were purified with a gel extraction method before being sequenced by Illumina MiSeq using V3 600 cycle reagents run as 270x12x12x270 at Penn State Genomics Core Facility. The sequencing reads were obtained and then processed by Qiime2 v2023.5 and Dada2 v1.26.0 for demultiplexing and denoising, respectively. The Greengenes2 database with clustering at 99% sequence similarity was utilized for taxonomy

assignments into kingdom, phylum, class, order, family, genus, and species levels by the QIIME2 classifier. The phylogenetic tree was constructed by using the QIIME2 phylogeny align-to-tree-mafft-fasttree tool. Alpha diversity was estimated using the observed ASVs, Shannon's diversity, and phylogenetic diversity after subsampling to the lowest sequencing ddepth; whereas beta diversity was analyzed using Bray Curtis dissimilarity, CLR Euclidean (Aitchison) distance, weighted, and unweighted UniFrac distance metrics. Shannon diversity was calculated using the R package vegan v2.6-6.1 (41), while observed ASVs and phylogenetic diversity were calculated by picante v1.8.2 (42). The Bray Curtis dissimilarity was obtained by vegdist function (vegan v2.6-6.1), and then the CLR Euclidean distance was calculated by performing a centered log2 ratio transformation using make_clr (qiime2R v0.99.6). The weighted and unweighted UniFrac metrics were acquired by unifrac function (rbiom v1.0.3).

In vitro growth curve analysis of microbes

Liquid cultures of strains were prepared in BHI CHV media (Brain Heart Infusion with 5% w/v Cysteine, 5 mg/mL hemin, and 1 mg/mL vitamin K3) and incubated at 37°C in an anaerobic chamber with 20% CO_2, 5% H_2, and 75% N_2 gas for 48 hours (Coy Anaerobic Systems). The 83 strains were subcultured (1:100) into BHI CHV containing BRB (160 µg/mL in water), or BHI CHV containing DBP (1µM in DMSO) on a 96-well plate which was shaken for 30 seconds before reading with a 15-minute interval. The OD values were detected by a BioTek Epoch2 plate reader. After 72 hours, the data was exported by the Gen5 software (version 3.13.15) and normalized by subtracting the OD values of the pure culture. Each assay was run in quadruplicates. The growth curve parameters were calculated with a Growthcurver v0.3.1 R package which fits the data to a logistic equation describing the population size N_t at time t using:

$$N_t = \frac{K}{1 + (\frac{K - N_0}{N_0})e^{-rt}}$$

Wherein N_0 is the population size at the start point, K represents the maximum possible population size or carrying capacity, and r stands for the intrinsic growth rate. Additionally, an output metric, t-mid reports the time when the population density reaches $\frac{1}{2}K$. In the current study, the carrying capacity k, the growth rate r, and the time to reach half carrying capacity t-mid for each strain were obtained to evaluate the growth condition.

Statistical analysis

All statistics were analyzed in R version 4.3.3 using a two-factor ANOVA including the BRB effect, DBP effect, and BRB*DBP interaction unless otherwise noted. Beta diversity differences and homogeneity of multivariate dispersions were analyzed by Adonis (PERMANOVA) and Betadisper (PERMDISP), respectively, with vegan v 2.6-6.1 package. Differentially abundant microbes were analyzed by using the aldex.glm and aldex.glm.effect functions from the ALDEx2 v1.24.0 package. In the comparisons between DBP vs DMSO groups using ALDEx2, Welch's t-test FDR-corrected P values were carried forward. The growth curve parameters were analyzed using an FDR-corrected Wilcoxon rank sum test to detect significant differences.

Data availability

The raw sequencing data generated in this study are publicly available at NCBI Sequence Read Archive (SRA) under accession PRJNA1142100.

RESULTS

DBP-induces DNA damage

We conducted a mouse experiment in which 5-week-old individually-housed female B6C3F1 mice were randomly assigned into four groups (N=5 per group): (1) DMSO; (2) DBP; (3) BRB; and (4) BRB+DBP (**Fig. 1a**). The mice in DMSO and DBP groups were fed AIN-93M control diet, whereas those in BRB and BRB+DBP groups received AIN-93M control diet containing 5% w/w BRB. We treated the mice in DMSO and BRB groups with DMSO (vehicle) or topically applied 24 nmol DBP into the oral cavity of the mice three times a week for 5-6 weeks. Mouse oral and cecal samples were collected after the last dose of carcinogen administration. DNA damage is an essential step in the initiation of OSCC in mice treated with DBP (26–28). After the collection of oral samples, the oral tissues were harvested to examine the levels of DNA adducts derived from DBP (DBPDE-dA). Although no histological changes at this early time point are observed in this model (26,35), DBPDE-dA was detected in the DBP group at the level of 0.495 ± 0.021 adducts per 10^6 deoxyadenosine (dA) by using an LC-MS/MS with stable isotope dilution assay, confirming the capacity of DBP to trigger DNA damage. Representative LC-MS/MS chromatographs for DBPDE-dA and the reference standard ^{15}N-DBPDE-dA are shown in **Fig. 1b** and **Fig. 1c**, respectively. Consistent with our previous reports, the adduct was not detected in mice treated with DMSO (26,43).

BRB consumption reshapes the gut microbiota whereas DBP shows no effect

Since the microbiome is associated with the development of oral cancer (5,6) and we have previously shown protective effects of BRB against DBP-mediated OSCC (35), we sequenced a total of 20 cecal samples which resulted in 611,815 reads after processing (30,590.8 ± 6,582.6 per sample (mean ± sd)). The BRB treatment significantly increased the microbial richness represented by the number of observed Amplicon sequence variants (ASVs) compared to the non-BRB treatment, while DBP showed no significant effect (**Fig. 2a**). The number of ASVs observed in the control groups ranged from (91.5 [77-108]; median [range]), which was significantly decreased compared to the BRB treated mice (150 [138-161]; P=4.0e-7, two-factor ANOVA). This observation was also true of phylogenetic diversity, and Shannon's diversity metrics (P=1.5e-6 and P=7.4e-4, respectively). The gut microbial composition, represented by PCoA (Principal Coordinate Analysis) analysis of Bray Curtis dissimilarity identified a significant effect of BRB (P=0.001, R^2=0.28) but not DBP (P=0.32) or an interaction between DBP and BRB (P=0.63; **Fig. 2b;** PERMANOVA/ADONIS). This observation of a significant effect of BRB was robust to distance metric choice also being significant for CLR Euclidean, weighted UniFrac, and unweighted UniFrac metrics (P=0.001, P=0.002, and P=0.001 respectively). Taken together, these observations illustrate that BRB consumption, irrespective of DBP exposure, leads to a distinct gut microbiome composition.

Compared to vehicle (DMSO) and DBP groups, BRB and BRB+DBP groups also shifted the compositional structure of the microbiome at the family level, characterized by a reduction in the relative abundance of *Akkermansiaceae* (**Fig. 2c**). *Muribaculaceae* and *Lachnospiraceae* were the two most prominent families in the gut bacterial community, constituting 71.8 ± 6.7% of the community. Next, we applied a generalized linear model using ALDEx2 to identify the differentially abundant ASVs and detected a significant effect of BRB (FDR<0.1) on 17 ASVs (**Fig. 2d**) but no ASVs displaying a significant effect of DBP or interaction (all FDR>=0.1). *A. muciniphila*, *Oscillospiraceae spp.*, *Dysosmobacter spp.*, *Angelakisella massiliensis*, *Lachnospiraceae spp.*, *Lawsonibacter spp.*, and *Acutalibacter muris* were significantly decreased after BRB treatment compared with non-BRB treatment. In contrast, BRB treatment resulted in the enrichment of the ASVs *Lawsonibacter sp.*, *Dysosmobacter sp.*, *Eubacterium sp.*, *Schaedlerella arabinosiphila*, *Emergencia sp.*,

Anaerovoracaceae sp., *Kineothrix sp.*, *Ruminococcus sp.*, and *Oscillospiraceae sp.* To dissociate the effects of BRB only, we replicated our analysis using only the BRB and DMSO groups which had not been treated with BRB, confirming the decrease of *A. muciniphila* in mice treated with BRB (**Fig. 2e**). In addition, significantly elevated levels of *Kineothrix sp.*, *Schaedlerella arabinosiphila*, and *Eubacterium sp.* and reduced abundance of *Oscillospiraceae sp.*, *Angelakisella massiliensis*, *Acutalibacter muris*, and *Lachnospiraceae sp.* were also observed in BRB group relative to DMSO group. Consistent with our analyses, the relative abundance of the *Akkermansia* genus was significantly reduced after BRB treatment (**Fig. 2f**).

BRB exhibits significant but limited effects on oral microbiota

The presence of BRB-associated bioactive compounds may be more transient in the oral cavity than the gut given temporal variation in eating behavior and frequent swallowing behavior. Given this, we next sought to investigate how BRB and DBP impact the oral microbiome. Similarly, a total of 20 oral samples sequenced targeting the V4 region of the 16S rRNA gene. After processing, we obtained 640,437 total reads with 32,021.9 ± 20,698.7 reads per sample. Unlike the gut, there was no significant effect of BRB, DBP, or their interaction on the oral bacterial diversity based on the alpha diversity analysis using Observed ASVs with 53 [32-111] ASVs in Control and 47.5 [25-90] ASVs in BRB ($P>0.05$; two-way ANOVA test; median [range]; **Fig. 3a**). The number of observed ASVs ranged from a median of 48.7 [25-111] in the oral microbiota which was significantly lower relative to that in the gut microbiota with 125.5 [77-179] ASVs (P=1.8e-4; Wilcoxon Signed Rank test; **Fig. S1**). Nevertheless, the analysis of Bray Curtis dissimilarity revealed a significant effect of BRB (P=0.024, R^2=0.12) but not DBP (P=0.24, R^2=0.062) or their interaction (P=0.31, R^2=0.058; **Fig. 3b**), further emphasizing that BRB exerted greater influence on the microbiome than DBP. The result was validated by other beta diversity metrics CLR Euclidean and unweighted UniFrac (P=0.001 and P=0.012, respectively).

A bar plot of family-level relative abundances shows heterogeneity within groups and with minor taxonomic differences between groups including a decrease in *Enterococcaceae* in the DBP-treated group (**Fig.3c**). High relative abundances of *Akkermansiaceae* were observed in several samples of the non-BRB compared to BRB groups (P=0.011, two-way ANOVA test). Interestingly, high abundances of *Akkermansiaceae* were detected in the DMSO group from both cecal (**Fig. 2c**) and oral (**Fig. 3c**) samples suggesting high baseline levels of *Akkermansiaceae* possibly due to vendor variation (44) or dietary factors (45). No differentially abundant microbes were detected between groups except that an ASV belonging to the *Rickettsiales* which may be derived from the host mitochondria and was different between the DMSO and BRB groups (**Fig. 3d**). Although *A. muciniphila* was lower in the DMSO group, the effect was not significant after multiple testing correction at the ASV level (FDR>0.1). However, when genus level abundances were considered, only a significant BRB effect (P=0.0025; two-way ANOVA test) was detected, showing reduced *Akkermansia* after BRB treatment (**Fig. 3e**), which is consistent with that in the gut. In addition, the genus belonging to the opportunistic pathogen *Enterococcus* (46) was significantly reduced after BRB treatment, but no significant DBP or interaction effect was detected (**Fig. 3f**).

BRB selectively modifies microbial growth *in vitro*

At an early time point prior to the detection of any histological changes in the mouse oral cavity, our *in vivo* experiments in mice revealed that BRB significantly modified the gut and oral microbes while DBP had no effect, we next sought to apply *in vitro* models with human microbes to replicate our *in vivo* findings from animal models. A total of 83 bacterial strains, selected to represent a diversity of human commensals, were cultured in rich media containing 160 µg/mL of BRB or 1 µM of DBP for 72 hours. The doses were selected according to our previous studies showing that BRB had dose-dependent

protections against DBP-induced DNA damage in human and rat oral cells (47,48). The growth of each strain is represented by parameters extracted from a logistic growth model (49) and compared between vehicle control and treatment groups. The addition of BRB enhanced the growth of *Lactobacillus paracasei JEB00396*, characterized by significantly elevated carrying capacity (**Fig. 4a**). In addition, the growth rates of *Leuconostoc lactis JEB00394*, *Parabacteroides goldsteinii JEB00421*, and *Bacteroides finegoldii JEB00452* were significantly increased (Wilcoxon rank sum test, FDR<0.05, |log2 fold change|>0.5), suggesting that BRB favors the growth of some microbes. In contrast, *Bifidobacterium adolescentis JEB00411* showed a declined growth rate after BRB treatment, indicating a potential inhibitory effect. The increased growth rate of *Leuconostoc lactis JEB00394* by BRB was also demonstrated by the decrease in t-mid (time to reach half carrying capacity). Next, we turned to investigate the effect of DBP. Consistent with *in vivo* studies, there were no significant effects for any tested strain treated with DBP (**Fig. 4b**).

To further examine the *in vivo* finding that BRB decreased the abundance of *A. muciniphila*, we replicated the experiment to test the effect of BRB and DBP on two *A. muciniphila* strains. Countering *in vivo* observations, after 72 hours of incubation, the BRB group showed minor increases in growth (**Fig. S2**). This suggests that while *A. muciniphila* may utilize BRB substrates *in vitro,* the mechanism of inhibition *in vivo* may involve host-microbe and microbe-microbe interactions not captured in mono-culture.

Discussion

The gut and oral microbiota constitute two of the highest biomass microbial ecosystems within the human body (50), characterized by diverse composition and ecological dynamics (51). Anatomically contiguous through the gastrointestinal tract and linked chemically via saliva and ingested food transit (52), the oral-gut microbiome axis has been implicated in various disease processes (53). In our study, we examined both oral and gut microbiota, at early time points prior to any morphological changes associated with cancer to elucidate their response to DBP-induced tumorigenesis. No significant effect of DBP on microbial composition was detected either *in vivo* or *in vitro*, suggesting that the carcinogen may have a little direct effect on the microbiome relative to the host environment; however, the possibility remains that microbes could respond to subtle changes in the micro-environment especially under abnormal conditions (54), thereby serving biosensors for cancer detection Although studies that explored the DBP-microbiome interaction are scarce, benzo[a]pyrene (B[a]P), another PAH, was reported to alter the structure of the gut microbiota in a murine model after 28-day oral gavage (55); such an effect was not replicated in human gut microbiota using an *in vitro* assay, despite that the volatile metabolome and transcriptome were influenced by B[a]P which may suggest that microbial metabolic activity is modulated without impacting community composition (56).

Treating cancers at late stage, including OSCC continues to be a major challenge and thus, development of safe and effective strategies for cancer prevention remains a desirable approach. Consumption of diets rich in fruits and vegetables may lower the risk of developing OSCC and foods (e.g. BRB) that contain agents known to inhibit the initiation and/or progression of the multi-step carcinogenesis process are favorable candidates for cancer prevention (20,29). Consistent with previous findings in murine models (36,57–60) and human gut microbiota studies *in vitro* (61,62), dietary BRB significantly modified the microbial diversity of the gut microbiota, underscoring the potent role of dietary intervention in microbiome modulation. Mice on the BRB diet exhibited increased ASV richness in the gut microbiome compared to controls, suggesting potential beneficial effects, as lower microbial diversity is associated with acute and chronic diseases (63). In both the gut and the oral microbiome, a high relative abundance of the family *Akkermansiaceae* was detected in the control

group. In a previous mouse model study, a BRB diet (10% w/w for 7 weeks) increased the abundance of *A. muciniphila* in the gut; however, the oral cavity was not explored (36). Based on our previous findings, the cancer preventive action of BRB is optimal at 5% in the diet and no additional advantages were gained when BRB was used at 10% (20). The ability of BRB to modulate microbial growth was also detected in our *in vitro* model which describes a more direct relationship between BRB and *A. muciniphila*. Contrasting to high baseline *A. muciniphila* levels in our *in vivo* models, the control group in the previous research only had <0.01% *A. muciniphila* in the community (36), further suggesting that BRB may indirectly impact *A. muciniphila* through complex host-microbe and microbe-microbe interactions *in vivo*. In addition to *A. muciniphila*, reduced levels of *Acutalibacter muris*, *Angelakisella massiliensis*, *Dysosmobacter spp.*, and *Oscillospiraceae spp.,* all belonging to the family *Oscillospiraceae* were observed following BRB treatment. Interestingly, *Acutalibacter muris* has been identified as a biomarker of colorectal cancer (64) and lung cancer (65), suggesting that BRB may mitigate cancer development through microbial modulation. On the other hand, the presence of dietary BRB resulted in significantly more abundant *Eubacterium sp.*, *Schaedlerella arabinosiphila*, and *Kineothrix sp*.. *Eubacterium callanderi* has demonstrated anti-colorectal cancer properties both *in vitro* and *in vivo*, potentially mediated by metabolites such as butyrate and 4-aminobutanoic acid (66), whereas *Kineothrix alysoides* is known to produce butyrate (67), demonstrating that BRB may selectively promote butyrate-producers resulting in suppressed carcinogenic potential (68). Our *in vitro* experiments showed that BRB promoted the proliferation of the microbes potentially involved in polyphenol metabolism: two lactic acid bacterial strains (69) and two *Bacteroidotas* (62). Among them, *Lactobacillus paracasei* has been reported to exert anti-proliferative and apoptotic effects in human colon cancer cells (70,71) and cervix cancer cells (72,73), while *Parabacteroides goldsteinii* has been noted for its anti-inflammatory properties through its lipopolysaccharide (74) and anti-virulence factor functions (75), underscoring their potential therapeutic relevance.

In the present study, we used female mice since we showed that the histological and molecular characteristics in the mouse oral cavity following DBP treatment mimic the human disease; nevertheless, the lack of information in male mice is considered a limitation. Thus, future investigations are needed to identify the causal role of the altered microbiome in the development or prevention of DBP-induced OSCC in both sexes. The alteration in *A. muciniphila* following BRB treatment was observed; however, its specific influence on OSCC development remains unclear. To gain insights into the mechanism involved, it will be necessary to isolate the representative strains and employ further animal models to examine causality at different stages of disease during the multi-step carcinogenesis process from normal, dysplasia, carcinoma *in situ*, and OSCC. Additionally, the integration of metabolomics analyses may provide new insights into the role of microbial metabolites derived from BRB and DBP in carcinogenesis. Conventional mouse and germ-free mouse models may enable us to identify candidate metabolites and further mechanistic analysis with such metabolites is warranted to quantify their effect on carcinogenesis.

Overall, this work extends our prior mechanistic investigations (35) for BRB modulation in DBP-induced OSCC, focusing on the microbial perspective. We have provided evidence that BRB not only affects the structure of the gut microbiome but also induces changes in the composition of oral microbial communities in the context of DBP-induced DNA damage. Continued progress in elucidating carcinogen-microbiome interaction could help the development of microbial-based strategies for cancer prevention.

Acknowledgments

J. Zhao: investigation, methodology, formal analysis, visualization, data curation, writing—original draft, writing—review and editing. **Y-W. Sun**: conceptualization; DNA isolation from oral tissues, and writing original draft. **K-M. Chen**: LC-MS/MS analysis of DNA adducts derived from DBP. **C. Aliaga**: animal handling, carcinogen treatment, diet preparation, animal sacrifice, oral, cecal and tissue collection. **J.E. Bisanz**: Conceptualization, formal analysis, methodology, validation, supervision, writing–original draft, writing–review and editing. **K. El-Bayoumy**: Conceptualization, formal analysis, funding acquisition, methodology, writing–original draft, project administration, writing–review and editing. JEB is supported by NIGMS R35 GM151045 and funds provided by the Huck Institute for the Life Sciences. KEB: This study is supported in part by NCI R01 CA173465.

References

1. Sung H, Ferlay J, Siegel R, Laversanne M, Soerjomataram I, Jemal A, et al. Global cancer statistics 2020: GLOBOCAN estimates of incidence and mortality worldwide for 36 cancers in 185 countries. CA Cancer J Clin. 2021;71:209–49.

2. Siegel RL, Giaquinto AN, Jemal A. Cancer statistics, 2024. CA Cancer J Clin. pinchnews.com; 2024;74:12–49.

3. Liu H, Huang Y, Huang M, Huang Z, Wang Q, Qing L, et al. Current status, opportunities, and challenges of exosomes in oral cancer diagnosis and treatment. Int J Nanomedicine. Informa UK Limited; 2022;17:2679–705.

4. Abati S, Bramati C, Bondi S, Lissoni A, Trimarchi M. Oral Cancer and Precancer: A Narrative Review on the Relevance of Early Diagnosis. Int J Environ Res Public Health. 2020;17:9160.

5. Chen J, Domingue JC, Sears CL. Microbiota dysbiosis in select human cancers: Evidence of association and causality. Semin Immunol. 2017;32:25–34.

6. Pignatelli P, Romei FM, Bondi D, Giuliani M, Piattelli A, Curia MC. Microbiota and Oral Cancer as A Complex and Dynamic Microenvironment: A Narrative Review from Etiology to Prognosis. Int J Mol Sci. 2022;23:8323.

7. Binder Gallimidi A, Fischman S, Revach B, Bulvik R, Maliutina A, Rubinstein AM, et al. Periodontal pathogens Porphyromonas gingivalis and Fusobacterium nucleatum promote tumor progression in an oral-specific chemical carcinogenesis model. Oncotarget. 2015;6:22613–23.

8. Kavarthapu A, Gurumoorthy K. Linking chronic periodontitis and oral cancer: A review. Oral Oncol. 2021;121:105375.

9. Hajishengallis G, Lamont RJ. Beyond the red complex and into more complexity: the polymicrobial synergy and dysbiosis (PSD) model of periodontal disease etiology. Mol Oral Microbiol. Wiley; 2012;27:409–19.

10. Whitmore SE, Lamont RJ. Oral bacteria and cancer. PLoS Pathog. Public Library of Science (PLoS); 2014;10:e1003933.

11. Sharma AK, DeBusk WT, Stepanov I, Gomez A, Khariwala SS. Oral Microbiome Profiling in Smokers with and without Head and Neck Cancer Reveals Variations Between Health and Disease. Cancer Prev Res . 2020;13:463–74.

12. Yang C-Y, Yeh Y-M, Yu H-Y, Chin C-Y, Hsu C-W, Liu H, et al. Oral Microbiota Community Dynamics Associated With Oral Squamous Cell Carcinoma Staging. Front Microbiol. 2018;9:862.

13. Healy CM, Moran GP. The microbiome and oral cancer: More questions than answers. Oral Oncol. 2019;89:30–3.

14. Perera M, Al-Hebshi NN, Perera I, Ipe D, Ulett GC, Speicher DJ, et al. Inflammatory Bacteriome and Oral Squamous Cell Carcinoma. J Dent Res. 2018;97:725–32.

15. Moon J-H, Lee J-H. Probing the diversity of healthy oral microbiome with bioinformatics approaches. BMB Rep. 2016;49:662–70.

16. Schwabe RF, Jobin C. The microbiome and cancer. Nat Rev Cancer. 2013;13:800–12.

17. Mager DL, Haffajee AD, Devlin PM, Norris CM, Posner MR, Goodson JM. The salivary microbiota

as a diagnostic indicator of oral cancer: a descriptive, non-randomized study of cancer-free and oral squamous cell carcinoma subjects. J Transl Med. 2005;3:27.

18. Hasan NA, Young BA, Minard-Smith AT, Saeed K, Li H, Heizer EM, et al. Microbial community profiling of human saliva using shotgun metagenomic sequencing. PLoS One. 2014;9:e97699.

19. Yang Y, Zheng W, Cai Q-Y, Shrubsole MJ, Pei Z, Brucker R, et al. Cigarette smoking and oral microbiota in low-income and African-American populations. J Epidemiol Community Health. 2019;73:1108–15.

20. El-Bayoumy K, Chen K-M, Zhang S-M, Sun Y-W, Amin S, Stoner G, et al. Carcinogenesis of the Oral Cavity: Environmental Causes and Potential Prevention by Black Raspberry. Chem Res Toxicol. 2017;30:126–44.

21. Macgregor ID. Effects of smoking on oral ecology. A review of the literature. Clin Prev Dent. 1989;11:3–7.

22. Wu J, Peters BA, Dominianni C, Zhang Y, Pei Z, Yang L, et al. Cigarette smoking and the oral microbiome in a large study of American adults. ISME J. 2016;10:2435–46.

23. Maki KA, Ganesan SM, Meeks B, Farmer N, Kazmi N, Barb JJ, et al. The role of the oral microbiome in smoking-related cardiovascular risk: a review of the literature exploring mechanisms and pathways. J Transl Med. 2022;20:584.

24. Kramer IR, Lucas RB, Pindborg JJ, Sobin LH. Definition of leukoplakia and related lesions: an aid to studies on oral precancer. Oral Surg Oral Med Oral Pathol. 1978;46:518–39.

25. Johnson DE, Burtness B, Leemans CR, Lui VWY, Bauman JE, Grandis JR. Head and neck squamous cell carcinoma. Nat Rev Dis Primers. 2020;6:92.

26. Guttenplan JB, Kosinska W, Zhao Z-L, Chen K-M, Aliaga C, DelTondo J, et al. Mutagenesis and carcinogenesis induced by dibenzo[a,l]pyrene in the mouse oral cavity: a potential new model for oral cancer. Int J Cancer. 2012;130:2783–90.

27. Chen K-M, Guttenplan JB, Zhang S-M, Aliaga C, Cooper TK, Sun Y-W, et al. Mechanisms of oral carcinogenesis induced by dibenzo[a,l]pyrene: an environmental pollutant and a tobacco smoke constituent. Int J Cancer. 2013;133:1300–9.

28. Chen K-M, Sun Y-W, Kawasawa YI, Salzberg AC, Zhu J, Gowda K, et al. Black Raspberry Inhibits Oral Tumors in Mice Treated with the Tobacco Smoke Constituent Dibenzo(def,p)chrysene Via Genetic and Epigenetic Alterations. Cancer Prev Res . 2020;13:357–66.

29. El-Bayoumy K, Christensen ND, Hu J, Viscidi R, Stairs DB, Walter V, et al. An Integrated Approach for Preventing Oral Cavity and Oropharyngeal Cancers: Two Etiologies with Distinct and Shared Mechanisms of Carcinogenesis. Cancer Prev Res . 2020;13:649–60.

30. Stairs DB, Landmesser ME, Aliaga C, Chen K-M, Sun Y-W, El-Bayoumy K. Black raspberry restores the expression of the tumor suppressor p120ctn in the oral cavity of mice treated with the carcinogen dibenzo[a,l]pyrene diol epoxide. PLoS One. Public Library of Science; 2021;16:e0259998.

31. Christensen ND, Chen K-M, Hu J, Stairs DB, Sun Y-W, Aliaga C, et al. The environmental pollutant and tobacco smoke constituent dibenzo [def, p] chrysene is a co-factor for malignant progression of mouse oral papillomavirus infections. Chem Biol Interact. Elsevier; 2021;333:109321.

32. Chen K-M, Sun Y-W, Krebs NM, Sun D, Krzeminski J, Reinhart L, et al. Detection of DNA adducts

derived from the tobacco carcinogens, benzo[a]pyrene and dibenzo[def,p]chrysene in human oral buccal cells. Carcinogenesis. Oxford Academic; 2022;43:746–53.

33. Mauceri R, Coppini M, Vacca D, Bertolazzi G, Panzarella V, Di Fede O, et al. Salivary Microbiota Composition in Patients with Oral Squamous Cell Carcinoma: A Systematic Review. Cancers. 2022;14:5441.

34. Pietrobon G, Tagliabue M, Stringa LM, De Berardinis R, Chu F, Zocchi J, et al. Leukoplakia in the Oral Cavity and Oral Microbiota: A Comprehensive Review. Cancers. 2021;13:4439.

35. Sami A, Elimairi I, Stanton C, Ross RP, Ryan CA. The Role of the Microbiome in Oral Squamous Cell Carcinoma with Insight into the Microbiome–Treatment Axis. Int J Mol Sci. Multidisciplinary Digital Publishing Institute; 2020;21:8061.

36. Tu P, Bian X, Chi L, Gao B, Ru H, Knobloch TJ, et al. Characterization of the Functional Changes in Mouse Gut Microbiome Associated with Increased Akkermansia muciniphila Population Modulated by Dietary Black Raspberries. ACS Omega. 2018;3:10927–37.

37. Baker JL, Mark Welch JL, Kauffman KM, McLean JS, He X. The oral microbiome: diversity, biogeography and human health. Nat Rev Microbiol. 2024;22:89–104.

38. Tan X, Wang Y, Gong T. The interplay between oral microbiota, gut microbiota and systematic diseases. J Oral Microbiol. 2023;15:2213112.

39. Abusleme L, Hong B-Y, Hoare A, Konkel JE, Diaz PI, Moutsopoulos NM. Oral Microbiome Characterization in Murine Models. Bio Protoc. 2017;7:e2655–e2655.

40. Gohl DM, Vangay P, Garbe J, MacLean A, Hauge A, Becker A, et al. Systematic improvement of amplicon marker gene methods for increased accuracy in microbiome studies. Nat Biotechnol. 2016;34:942–9.

41. Oksanen J, Blanchet FG, Kindt R, Legendre P, Minchin PR, O'hara RB, et al. Community ecology package. R package version. sortie-admin.readyhosting.com; 2013;2:321–6.

42. Kembel SW, Cowan PD, Helmus MR, Cornwell WK, Morlon H, Ackerly DD, et al. Picante: R tools for integrating phylogenies and ecology. Bioinformatics. 2010;26:1463–4.

43. Chen K-M, Guttenplan JB, Sun Y-W, Cooper T, Shalaby NAE, Kosinska W, et al. Effects of black raspberry on dibenzo[a,l]pyrene diol epoxide induced DNA adducts, Mutagenesis, and tumorigenesis in the mouse oral cavity. Cancer Prev Res (Phila). 2018;11:157–64.

44. Rasmussen TS, de Vries L, Kot W, Hansen LH, Castro-Mejía JL, Vogensen FK, et al. Mouse Vendor Influence on the Bacterial and Viral Gut Composition Exceeds the Effect of Diet. Viruses. 2019;11:435.

45. Verhoog S, Taneri PE, Roa Díaz ZM, Marques-Vidal P, Troup JP, Bally L, et al. Dietary Factors and Modulation of Bacteria Strains of Akkermansia muciniphila and Faecalibacterium prausnitzii: A Systematic Review. Nutrients. MDPI AG; 2019;11:1565.

46. Krawczyk B, Wityk P, Gałęcka M, Michalik M. The Many Faces of Enterococcus spp.—Commensal, Probiotic and Opportunistic Pathogen. Microorganisms. Multidisciplinary Digital Publishing Institute; 2021;9:1900.

47. Guttenplan JB, Chen K-M, Sun Y-W, Kosinska W, Zhou Y, Kim SA, et al. Effects of black raspberry extract and protocatechuic acid on carcinogen-DNA adducts and Mutagenesis, and oxidative stress in rat and human oral cells. Cancer Prev Res (Phila). 2016;9:704–12.

48. Chen K-M, Sun Y-W, Sun D, Gowda K, Amin S, El-Bayoumy K. Black raspberry extract enhances glutathione conjugation of the fjord-region diol epoxide derived from the tobacco carcinogen dibenzo[def,p]chrysene in human oral cells. Chem Res Toxicol. American Chemical Society (ACS); 2022;35:2152–9.

49. Sprouffske K, Wagner A. Growthcurver: an R package for obtaining interpretable metrics from microbial growth curves. BMC Bioinformatics. 2016;17:172.

50. Peterson J, Garges S, Giovanni M, McInnes P, Wang L, Schloss JA, et al. The NIH human microbiome project. Genome Res. Cold Spring Harbor Lab; 2009;19:2317–23.

51. Structure, function and diversity of the healthy human microbiome. Nature. Nature Publishing Group; 2012;486:207–14.

52. Schmidt TS, Hayward MR, Coelho LP, Li SS, Costea PI, Voigt AY, et al. Extensive transmission of microbes along the gastrointestinal tract. Elife. 2019;8:e42693.

53. Park S-Y, Hwang B-O, Lim M, Ok S-H, Lee S-K, Chun K-S, et al. Oral–Gut Microbiome Axis in Gastrointestinal Disease and Cancer. Cancers . Multidisciplinary Digital Publishing Institute; 2021;13:2124.

54. Pan M, Zhang M, Rong X-Y, Zhao C. Human microbiota alterations — emerging predictors of renal diseases and kidney-specific aging. Aging Pathobiol Ther. 2023;5:39–47.

55. Ribière C, Peyret P, Parisot N, Darcha C, Dechelotte P, Barnich N, et al. Oral exposure to environmental pollutant benzo[a]pyrene impacts the intestinal epithelium and induces gut microbial shifts in murine model. Sci Rep. 2016;6:1–11.

56. Defois C, Ratel J, Denis S, Batut B, Beugnot R, Peyretaillade E, et al. Environmental Pollutant Benzo[a]Pyrene Impacts the Volatile Metabolome and Transcriptome of the Human Gut Microbiota. Front Microbiol. 2017;8:1562.

57. Rodriguez DM, Hintze KJ, Rompato G, Van Wettere AJ, Ward RE, Phatak S, et al. Dietary supplementation with black raspberries altered the gut microbiome composition in a mouse model of colitis-associated colorectal cancer, although with differing effects for a healthy versus a Western basal diet. Nutrients. MDPI AG; 2022;14:5270.

58. Lim T, Lee K, Kim RH, Ryu J, Cha KH, Park SY, et al. Effects of black raspberry extract on gut microbiota, microbial metabolites, and expressions of the genes involved in cholesterol and bile acid metabolisms in rats fed excessive choline with a high-fat diet. Food Sci Biotechnol. 2023;32:577–87.

59. Gu J, Thomas-Ahner JM, Riedl KM, Bailey MT, Vodovotz Y, Schwartz SJ, et al. Dietary black raspberries impact the colonic microbiome and phytochemical metabolites in mice. Mol Nutr Food Res. Wiley; 2019;63:e1800636.

60. Pan P, Lam V, Salzman N, Huang Y-W, Yu J, Zhang J, et al. Black raspberries and their anthocyanin and fiber fractions alter the composition and diversity of gut Microbiota in F-344 rats. Nutr Cancer. 2017;69:943–51.

61. Zhang S, Xu M, Sun X, Liu X, Choueiry F, Xu R, et al. Black raspberry extract shifted gut microbe diversity and their metabolic landscape in a human colonic model. J Chromatogr B Analyt Technol Biomed Life Sci. 2022;1188:123027.

62. Chan Y-T, Huang J, Wong H-C, Li J, Zhao D. Metabolic fate of black raspberry polyphenols in

association with gut microbiota of different origins in vitro. Food Chem. 2023;404:134644.

63. Pickard JM, Zeng MY, Caruso R, Núñez G. Gut microbiota: Role in pathogen colonization, immune responses, and inflammatory disease. Immunol Rev. 2017;279:70–89.

64. Uppakarn K, Bangpanwimon K, Hongpattarakere T, Wanitsuwan W. Comparison of the human gut Microbiota between normal control subjects and patients with colonic polyps and colorectal cancer. 2021; Available from: https://pdfs.semanticscholar.org/dd59/8684925d1f49cbfb154507a17021f47c740c.pdf

65. Feng C, Li N, Gao G, He Q, Kwok L-Y, Zhang H. Dynamic Changes of the Gut Microbiota and Its Functional Metagenomic Potential during the Development of Non-Small Cell Lung Cancer. Int J Mol Sci. 2024;25:3768.

66. Ryu SW, Kim J-S, Oh BS, Choi WJ, Yu SY, Bak JE, et al. Gut Microbiota Eubacterium callanderi Exerts Anti-Colorectal Cancer Activity. Microbiol Spectr. 2022;10:e0253122.

67. Haas KN, Blanchard JL. Kineothrix alysoides, gen. nov., sp. nov., a saccharolytic butyrate-producer within the family Lachnospiraceae. Int J Syst Evol Microbiol. 2017;67:402–10.

68. O'Keefe SJD. Diet, microorganisms and their metabolites, and colon cancer. Nat Rev Gastroenterol Hepatol. Springer Science and Business Media LLC; 2016;13:691–706.

69. Piekarska-Radzik L, Klewicka E. Mutual influence of polyphenols and Lactobacillus spp. bacteria in food: a review. Eur Food Res Technol. 2021;247:9–24.

70. Chondrou P, Karapetsas A, Kiousi DE, Tsela D, Tiptiri-Kourpeti A, Anestopoulos I, et al. Lactobacillus paracasei K5 displays adhesion, anti-proliferative activity and apoptotic effects in human colon cancer cells. Benef Microbes. Brill; 2018;9:975–83.

71. Orlando A, Refolo MG, Messa C, Amati L, Lavermicocca P, Guerra V, et al. Antiproliferative and proapoptotic effects of viable or heat-killed Lactobacillus paracasei IMPC2.1 and Lactobacillus rhamnosus GG in HGC-27 gastric and DLD-1 colon cell lines. Nutr Cancer. 2012;64:1103–11.

72. Riaz Rajoka MS, Zhao H, Lu Y, Lian Z, Li N, Hussain N, et al. Anticancer potential against cervix cancer (HeLa) cell line of probiotic Lactobacillus casei and Lactobacillus paracasei strains isolated from human breast milk. Food Funct. Royal Society of Chemistry (RSC); 2018;9:2705–15.

73. Mosleh IS, Karami F, Salahshourifar I, Ebrahimi MT, Marvibaigi M. Investigating the effects of Lactobacillus acidophilus and Lactobacillus paracasei supernatant on cervical cancer cells. Physiol Pharmacol Physicians. 2023;27:426–34.

74. Lai H-C, Lin T-L, Chen T-W, Kuo Y-L, Chang C-J, Wu T-R, et al. Gut microbiota modulates COPD pathogenesis: role of anti-inflammatory Parabacteroides goldsteinii lipopolysaccharide. Gut. 2022;71:309–21.

75. Lai C-H, Lin T-L, Huang M-Z, Li S-W, Wu H-Y, Chiu Y-F, et al. Gut Commensal Parabacteroides goldsteinii MTS01 Alters Gut Microbiota Composition and Reduces Cholesterol to Mitigate Helicobacter pylori-Induced Pathogenesis. Front Immunol. 2022;13:916848.

Figure Legends

Fig. 1 | Experimental design and validation. a, Experimental design: Mice started being fed an AIN-93 M diet (5% corn oil) as the control diet or an AIN-93M diet containing BRB (5%) 2 weeks prior to being treated with DBP (24 nmol) or DMSO three times per week for 5 to 6 weeks. **b,** Representative LC-MS/MS chromatographs for DBPDE-dA detected in the DBP group. The marked peak with a retention time of 1.582 mins represents DBPDE-dA in the samples. **c,** Representative LC-MS/MS chromatographs for ^{15}N-DBPDE-dA, an isotope internal standard added before DNA hydrolysis.

Fig. 2 | BRB treatment significantly modifies the gut microbiome whereas DBP showed no effect. a, BRB significantly increased microbial diversity compared with non-BRB treatment while the DBP resulted in comparable richness to the DMSO control group. **b,** BRB treatment led to a significantly different microbial composition, while no significant effect of DBP or DBP + BRB interaction with BRB was observed (PCoA of Bray-Curtis dissimilarity). **c,** Family-summarized data revealed that the relative abundance of *Akkermansiaceae* is decreased in BRB and BRB+DBP groups. **d,** In a generalized linear model, a significant BRB effect was detected on 18 ASVs (FDR<0.1), among which *A. muciniphila* was decreased after BRB treatment, whereas no DBP or interaction effect was observed. **e,** Differential abundance analysis between DMSO and BRB groups revealed that *A. muciniphila* was significantly reduced in the BRB group. **f,** The relative abundance of the genus *Akkermansia* significantly declined after the BRB treatment compared to non-BRB treatment. N=5 mice housed individually in each group. Statistical testing by a two-way ANOVA test with Tukey HSD in panels a and f, Adonis (PERMANOVA) analysis in panel b, differential abundance analysis using a generalized linear model within the ALDEx2 framework in panel d, and ALDEx2 with FDR-corrected Welch's t-test in panel e. CLR = centered $\log_2$ ratio.

Fig. 3 | BRB shifts the composition of the oral microbiome and decreases the relative abundance of the genus *Akkermansia*. a, Both DBP (P=0.40) and BRB (P=0.64) showed no significant effect on microbial diversity (ASV richness). **b,** There was an effect of BRB on microbial composition but not DBP or their interaction (PCoA of Bray-Curtis dissimilarity). **c,** A family-summarized abundance plot showed a decrease in *Akkermansiaceae* after BRB treatment compared with DMSO and DBP groups. **d,** Differentially abundant ASVs in a generalized linear model contrasting BRB treatment to control. **e,** The abundance of the genus *Akkermansia* was significantly reduced after the BRB treatment. **f,** The BRB treatment significantly decreased the relative abundance of the genus Enterococcus_E. In panels a, e, and f, statistical analysis was performed by a two-way ANOVA test containing BRB, DBP, and BRB-DBP interaction followed by Tukey HSD. In panels b and d, the data was analyzed by Adonis (PERMANOVA) and ALDEx2 with FDR-corrected Welch's t-test, respectively.

Fig. 4 | BRB impacts bacterial strain growth of select strains *in vitro* while DBP exhibits no significant effect. a, BRB significantly increased the carrying capacity (k) of *Lactobacillus paracasei JEB00396*, increased the growth rate (r) of *Leuconostoc lactis JEB00394*, *Parabacteroides goldsteinii JEB00421*, and *Bacteroides finegoldii JEB00452*, and decreased the r of *Bifidobacterium adolescentis JEB00411*. For *Leuconostoc lactis JEB00394*, t-mid, the time at which the population density reaches half of the carrying capacity significantly declined after BRB treatment. **b,** DBP had no significant effect on the growth of the bacterial strains. N=4 in each panel. The statistical analysis was performed by an FDR-corrected Wilcoxon rank sum test with FDR < 0.05 and the absolute value of log2 fold change ≥ 0.5 as the threshold to judge significant differences. Bacterial strains are clustered by a phylogenetic tree and colored by phylum.

Fig. 1

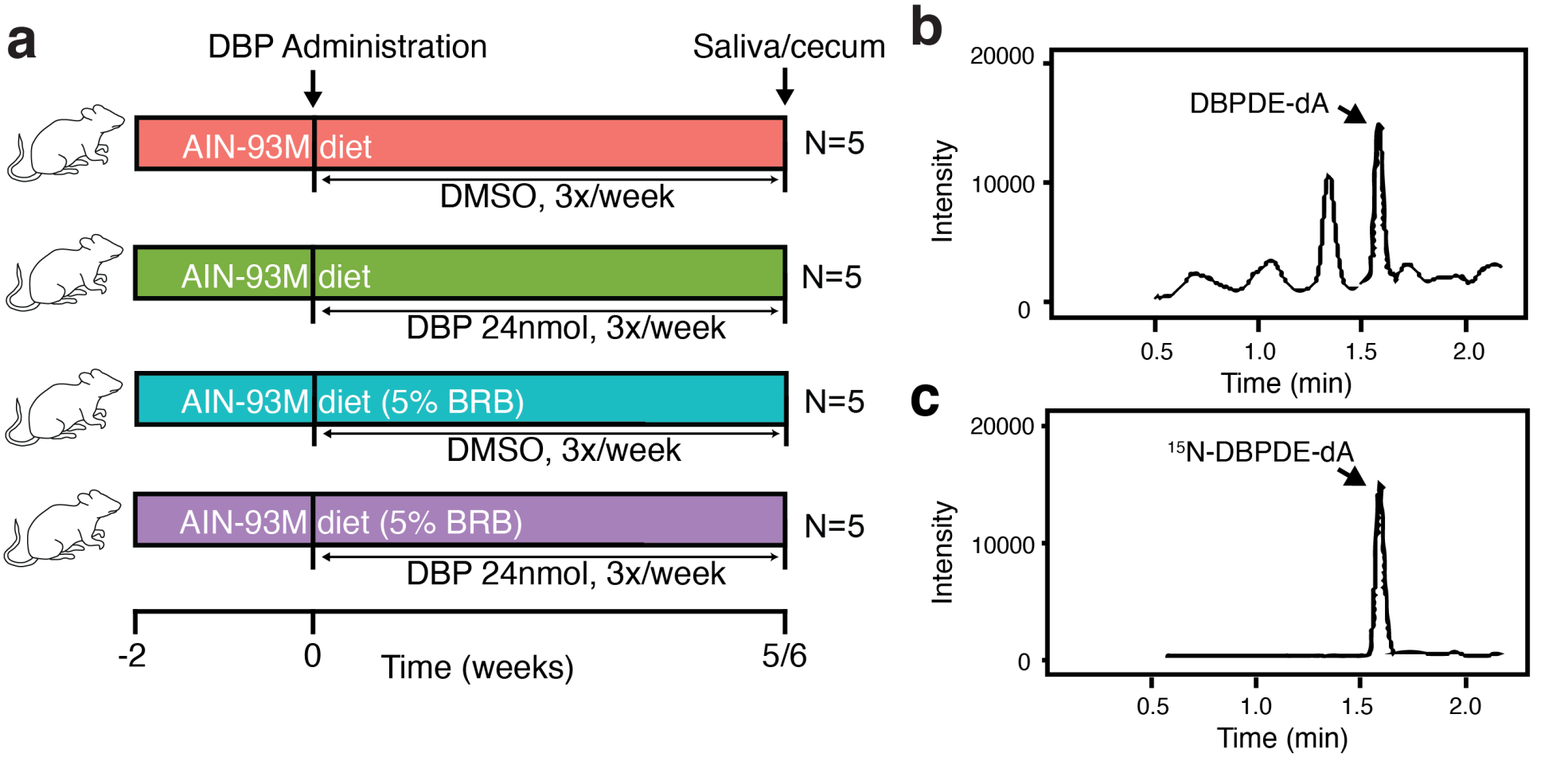
a
DBP Administration
Saliva/cecum
AIN-93M diet
DMSO, 3x/week
N=5
AIN-93M diet
DBP 24nmol, 3x/week
N=5
AIN-93M diet (5% BRB)
DMSO, 3x/week
N=5
AIN-93M diet (5% BRB)
DBP 24nmol, 3x/week
N=5
-2
0
5/6
Time (weeks)
b
DBPDE-dA
Intensity
20000
10000
0
0.5
1.0
1.5
2.0
Time (min)
c
15N-DBPDE-dA
Intensity
20000
10000
0
0.5
1.0
1.5
2.0
Time (min)

Fig. 2

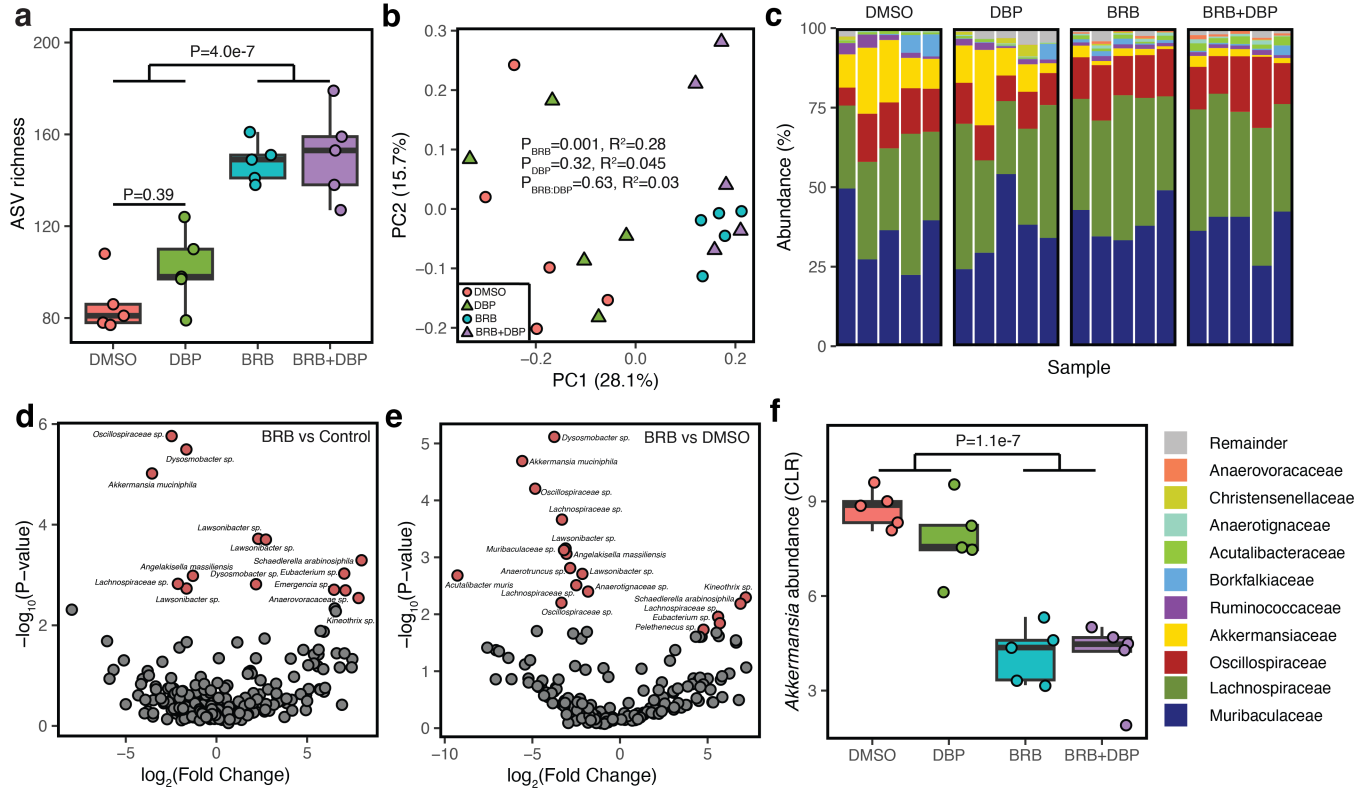
a
ASV richness
P=4.0e-7
P=0.39
DMSO
DBP
BRB
BRB+DBP
b
PC2 (15.7%)
PC1 (28.1%)
P_BRB=0.001, R²=0.28
P_DBP=0.32, R²=0.045
P_BRB:DBP=0.63, R²=0.03
DMSO
DBP
BRB
BRB+DBP
c
DMSO
DBP
BRB
BRB+DBP
Abundance (%)
Sample
d
BRB vs Control
−log10(P−value)
log2(Fold Change)
Oscillospiraceae sp.
Dysosmobacter sp.
Akkermansia muciniphila
Lawsonibacter sp.
Lawsonibacter sp.
Angelakisella massiliensis
Schaedlerella arabinosiphila
Lachnospiraceae sp.
Dysosmobacter sp. Eubacterium sp.
Emergencia sp.
Lawsonibacter sp.
Anaerovoracaceae sp.
Kineothrix sp.
e
BRB vs DMSO
−log10(P−value)
log2(Fold Change)
Dysosmobacter sp.
Akkermansia muciniphila
Oscillospiraceae sp.
Lachnospiraceae sp.
Lawsonibacter sp.
Muribaculaceae sp.
Angelakisella massiliensis
Anaerotruncus sp.
Lawsonibacter sp.
Acutalibacter muris
Lachnospiraceae sp.
Anaerotignaceae sp.
Kineothrix sp.
Schaedlerella arabinosiphila
Lachnospiraceae sp.
Oscillospiraceae sp.
Eubacterium sp.
Pelethenecus sp.
f
P=1.1e-7
Akkermansia abundance (CLR)
DMSO
DBP
BRB
BRB+DBP
Remainder
Anaerovoracaceae
Christensenellaceae
Anaerotignaceae
Acutalibacteraceae
Borkfalkiaceae
Ruminococcaceae
Akkermansiaceae
Oscillospiraceae
Lachnospiraceae
Muribaculaceae

Fig. 3

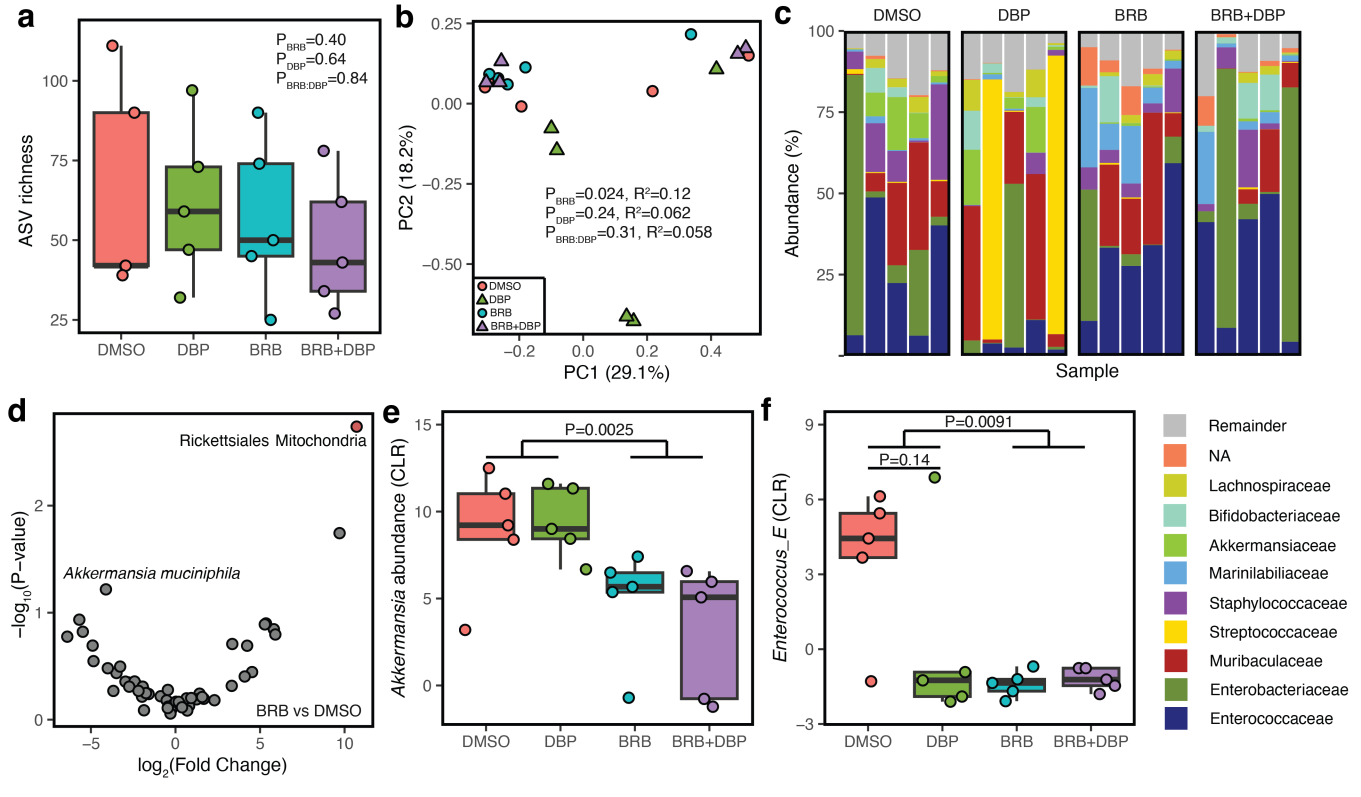
a
ASV richness
P_BRB=0.40
P_DBP=0.64
P_BRB:DBP=0.84
DMSO
DBP
BRB
BRB+DBP
b
PC2 (18.2%)
PC1 (29.1%)
P_BRB=0.024, R²=0.12
P_DBP=0.24, R²=0.062
P_BRB:DBP=0.31, R²=0.058
DMSO
DBP
BRB
BRB+DBP
c
Abundance (%)
Sample
d
Rickettsiales Mitochondria
Akkermansia muciniphila
BRB vs DMSO
−log10(P−value)
log2(Fold Change)
e
Akkermansia abundance (CLR)
P=0.0025
f
Enterococcus_E (CLR)
P=0.0091
P=0.14
Remainder
NA
Lachnospiraceae
Bifidobacteriaceae
Akkermansiaceae
Marinilabiliaceae
Staphylococcaceae
Streptococcaceae
Muribaculaceae
Enterobacteriaceae
Enterococcaceae

Fig. 4

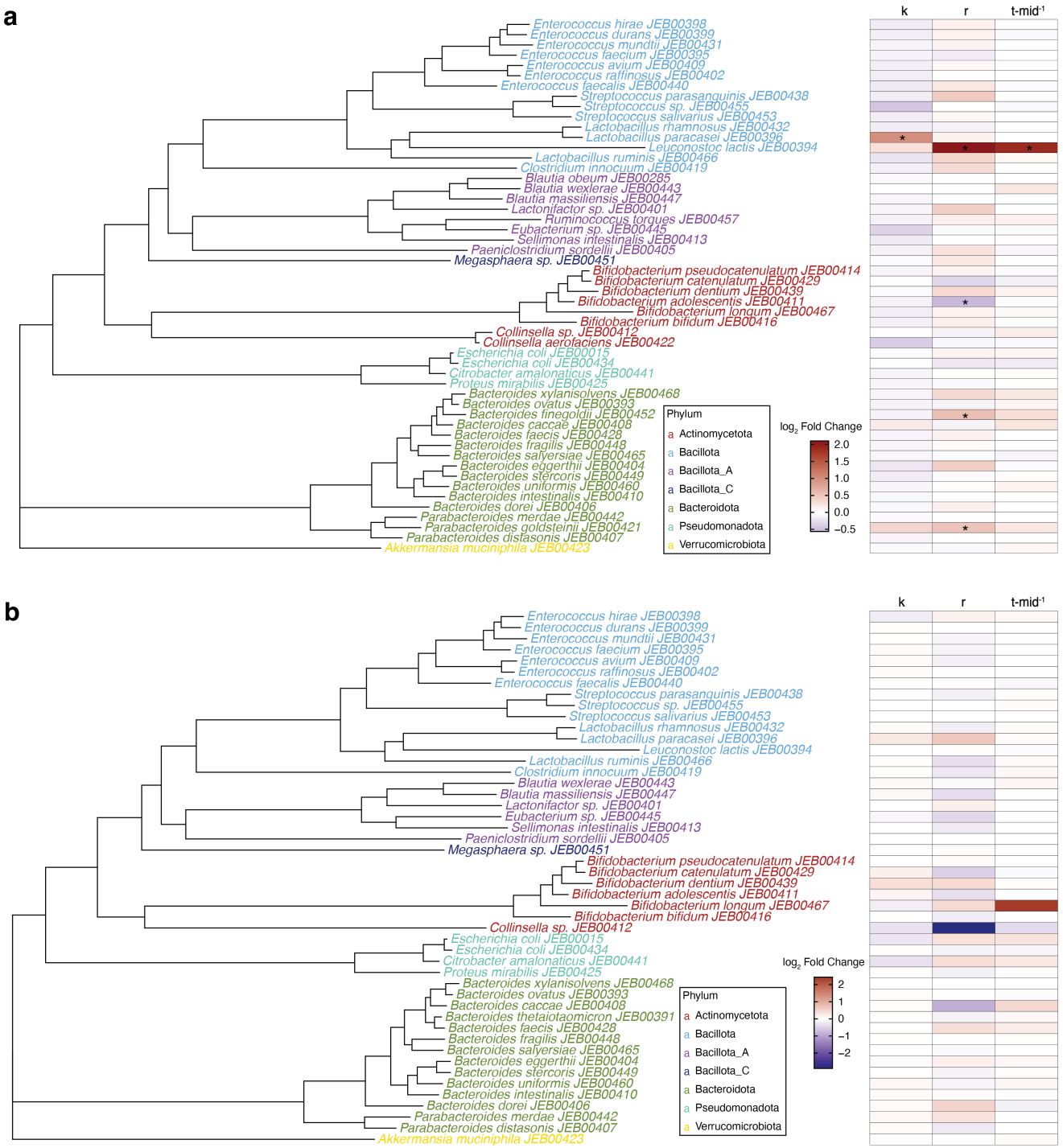
a
k
r
t-mid-1
Enterococcus hirae JEB00398
Enterococcus durans JEB00399
Enterococcus mundtii JEB00431
Enterococcus faecium JEB00395
Enterococcus avium JEB00409
Enterococcus raffinosus JEB00402
Enterococcus faecalis JEB00440
Streptococcus parasanguinis JEB00438
Streptococcus sp. JEB00455
Streptococcus salivarius JEB00453
Lactobacillus rhamnosus JEB00432
Lactobacillus paracasei JEB00396
Leuconostoc lactis JEB00394
Lactobacillus ruminis JEB00466
Clostridium innocuum JEB00419
Blautia obeum JEB00285
Blautia wexlerae JEB00443
Blautia massiliensis JEB00447
Lactonifactor sp. JEB00401
Ruminococcus torques JEB00457
Eubacterium sp. JEB00445
Sellimonas intestinalis JEB00413
Paeniclostridium sordellii JEB00405
Megasphaera sp. JEB00451
Bifidobacterium pseudocatenulatum JEB00414
Bifidobacterium catenulatum JEB00429
Bifidobacterium dentium JEB00439
Bifidobacterium adolescentis JEB00411
Bifidobacterium longum JEB00467
Bifidobacterium bifidum JEB00416
Collinsella sp. JEB00412
Collinsella aerofaciens JEB00422
Escherichia coli JEB00015
Escherichia coli JEB00434
Citrobacter amalonaticus JEB00441
Proteus mirabilis JEB00425
Bacteroides xylanisolvens JEB00468
Bacteroides ovatus JEB00393
Bacteroides finegoldii JEB00452
Bacteroides caccae JEB00408
Bacteroides faecis JEB00428
Bacteroides fragilis JEB00448
Bacteroides salyersiae JEB00465
Bacteroides eggerthii JEB00404
Bacteroides stercoris JEB00449
Bacteroides uniformis JEB00460
Bacteroides intestinalis JEB00410
Bacteroides dorei JEB00406
Parabacteroides merdae JEB00442
Parabacteroides goldsteinii JEB00421
Parabacteroides distasonis JEB00407
Akkermansia muciniphila JEB00423
Phylum
a Actinomycetota
a Bacillota
a Bacillota_A
a Bacillota_C
a Bacteroidota
a Pseudomonadota
a Verrucomicrobiota
log2 Fold Change
2.0
1.5
1.0
0.5
0.0
−0.5
b
k
r
t-mid-1
Enterococcus hirae JEB00398
Enterococcus durans JEB00399
Enterococcus mundtii JEB00431
Enterococcus faecium JEB00395
Enterococcus avium JEB00409
Enterococcus raffinosus JEB00402
Enterococcus faecalis JEB00440
Streptococcus parasanguinis JEB00438
Streptococcus sp. JEB00455
Streptococcus salivarius JEB00453
Lactobacillus rhamnosus JEB00432
Lactobacillus paracasei JEB00396
Leuconostoc lactis JEB00394
Lactobacillus ruminis JEB00466
Clostridium innocuum JEB00419
Blautia wexlerae JEB00443
Blautia massiliensis JEB00447
Lactonifactor sp. JEB00401
Eubacterium sp. JEB00445
Sellimonas intestinalis JEB00413
Paeniclostridium sordellii JEB00405
Megasphaera sp. JEB00451
Bifidobacterium pseudocatenulatum JEB00414
Bifidobacterium catenulatum JEB00429
Bifidobacterium dentium JEB00439
Bifidobacterium adolescentis JEB00411
Bifidobacterium longum JEB00467
Bifidobacterium bifidum JEB00416
Collinsella sp. JEB00412
Escherichia coli JEB00015
Escherichia coli JEB00434
Citrobacter amalonaticus JEB00441
Proteus mirabilis JEB00425
Bacteroides xylanisolvens JEB00468
Bacteroides ovatus JEB00393
Bacteroides caccae JEB00408
Bacteroides thetaiotaomicron JEB00391
Bacteroides faecis JEB00428
Bacteroides fragilis JEB00448
Bacteroides salyersiae JEB00465
Bacteroides eggerthii JEB00404
Bacteroides stercoris JEB00449
Bacteroides uniformis JEB00460
Bacteroides intestinalis JEB00410
Bacteroides dorei JEB00406
Parabacteroides merdae JEB00442
Parabacteroides distasonis JEB00407
Akkermansia muciniphila JEB00423
Phylum
a Actinomycetota
a Bacillota
a Bacillota_A
a Bacillota_C
a Bacteroidota
a Pseudomonadota
a Verrucomicrobiota
log2 Fold Change
2
1
0
−1
−2